The Journal of Experimental Biology 216, 4375-4387

doi:10.1242/jeb.092650

RESEARCH ARTICLE

Anoxia-mediated calcium release through the mitochondrial permeability transition pore silences NMDA receptor currents in turtle neurons

Peter John Hawrysh[1] and Leslie Thomas Buck[1,2,*]

[1]Department of Cell and Systems Biology and [2]Department of Ecology and Evolutionary Biology, University of Toronto, Toronto, ON, Canada, M5S 3G5

*Author for correspondence (les.buck@utoronto.ca)

SUMMARY

Mammalian neurons are anoxia sensitive and rapidly undergo excitotoxic cell death when deprived of oxygen, mediated largely by Ca^{2+} entry through over-activation of *N*-methyl-D-aspartate receptors (NMDARs). This does not occur in neurons of the anoxia-tolerant western painted turtle, where a decrease in NMDAR currents is observed with anoxia. This decrease is dependent on a modest rise in cytosolic $[Ca^{2+}]$ ($[Ca^{2+}]_c$) that is mediated by release from the mitochondria. The aim of this study was to determine whether the mitochondrial permeability transition pore (mPTP) is involved in NMDAR silencing through release of mitochondrial Ca^{2+}. Opening the mPTP during normoxia with atractyloside decreased NMDAR currents by releasing mitochondrial Ca^{2+}, indicated by an increase in Oregon Green fluorescence. Conversely, the mPTP blocker cyclosporin A prevented the anoxia-mediated increase in $[Ca^{2+}]_c$ and reduction in NMDAR currents. Mitochondrial membrane potential (Ψ_m) was determined using rhodamine-123 fluorescence and decreased with the onset of anoxia in a time frame that coincided with the increase in $[Ca^{2+}]_c$. Activation of mitochondrial ATP-sensitive potassium (mK^+_{ATP}) channels also releases mitochondrial Ca^{2+} and we show that activation of mK^+_{ATP} channels during normoxia with diazoxide leads to Ψ_m depolarization and inhibition with 5-hydroxydecanoic acid blocked anoxia-mediated Ψ_m depolarization. Ψ_m does not collapse during anoxia but rather reaches a new steady-state level that is maintained *via* ATP hydrolysis by the F_1-F_0 ATPase, as inhibition with oligomycin depolarizes Ψ_m further than the anoxic level. We conclude that anoxia activates mK^+_{ATP} channels, which leads to matrix depolarization, Ca^{2+} release *via* the mPTP, and ultimately silencing of NMDARs.

Key words: mitochondrial membrane potential, mitochondrial BK channel, pyramidal neurons, whole-cell patch-clamp, anoxia tolerance, channel arrest.

Received 17 June 2013; Accepted 21 August 2013

INTRODUCTION

The *N*-methyl-D-aspartate receptor (NMDAR) is a glutamatergic receptor found in the eukaryote brain and plays a crucial role in excitatory neurotransmission and learning and memory. Although it is widely considered to be one of the most fundamental neurotransmitter receptors in the brain, it can produce deleterious effects in response to overstimulation by glutamate. One such example of this is during oxygen deprivation in the mammalian brain, which results in rapid depolarization of neurons and excessive glutamate release. Because of its high calcium permeability, over-activation of NMDARs can lead to neurotoxic levels of intracellular calcium ($[Ca^{2+}]_i$), which can activate cell lipases, endonucleases, proteases and phosphatases, ultimately leading to the onset of excitotoxic cell death (Choi, 1992). However, sensitivity to oxygen deprivation has been overcome by certain vertebrates such as the western painted turtle [*Chrysemys picta bellii* (Gray 1831)], which can survive anoxic periods of over 4 months at 3°C (Ultsch and Jackson, 1982). This is made possible by a reduction in ATP-consuming reactions, such as Na^+/K^+-ATPase activity, which allows the cell to maintain [ATP] but must be matched by a coincident reduction in ion permeability (Buck and Hochachka, 1993). This phenomenon, known as 'channel arrest' (Hochachka, 1986), occurs following the onset of anoxia in turtle neurons and has been observed with several ion channels, such as the voltage-gated Na^+ channel, plasmalemmal K^+ channel, oxygen-sensitive calcium activated K^+ channels, and 2-amino-3-(3-hydroxy-5-methyl-isoxazol-4-yl)propanoic acid (AMPA) and NMDA receptors (Pérez-Pinzón et al., 1992; Pek-Scott and Lutz, 1998; Pamenter et al., 2008a; Buck and Bickler, 1995; Buck and Bickler, 1998; Shin and Buck, 2003; Rodgers-Garlick et al., 2013).

In addition to maintaining extracellular [glutamate] at basal levels through 5 h of anoxia (Thompson et al., 2007), turtle neurons regulate NMDAR activity through a reduction in channel open time; open probability is reduced by 65% after 60 min of anoxia (Buck and Bickler, 1998) and whole-cell NMDAR currents are reduced by 45–65% after 40 min of anoxia (Pamenter et al., 2008b; Shin and Buck, 2003; Bickler et al., 2000). These changes occur in a calcium-dependent manner: $[Ca^{2+}]_i$ levels increase by 35% following the onset of anoxia (Bickler et al., 2000) and inclusion of the Ca^{2+} chelator BAPTA [1,2-bis(o-aminophenoxy)ethane-*N*,*N*,*N*′,*N*′-tetraacetic acid] in the pipette solution of electrodes during whole-cell patch clamp experiments abolished the anoxia-mediated reduction in NMDAR currents (Pamenter et al., 2008b). The anoxia-mediated rise in Ca^{2+} occurs in the absence of extracellular Ca^{2+} and is hypothesized to be released from the mitochondria in response to activation of mitochondrial ATP-sensitive potassium (mK^+_{ATP}) channels, as application of the mK^+_{ATP} agonist diazoxide elevated $[Ca^{2+}]_i$ and application of the mK^+_{ATP} antagonist 5-

hydroxydecanoic acid (5-HD) abolished the anoxia-mediated rise in $[Ca^{2+}]_i$ (Pamenter et al., 2008b).

It is of interest to understand the mechanism of how a reduction of oxygen is transduced into a signal for mitochondrial Ca^{2+} release that leads to NMDAR silencing. There are a limited number of avenues through which Ca^{2+} can be transported across the inner mitochondrial membrane, the most often-cited mechanisms being the Na^+-dependent and -independent Ca^{2+} exchangers (Gunter et al., 2000; Nicholls and Budd, 2000). The Na^+-dependent Ca^{2+} transport is electrogenic and would therefore be influenced by perturbations in mitochondrial membrane potential (Ψ_m); the ionic ratio is hypothesized to be 3 Na^+ per 1 Ca^{2+} (Baysal et al., 1994). This would suggest that Ψ_m depolarization would drive this pathway to release positive charge from the mitochondria, resulting in 3 Na^+ out and 1 Ca^{2+} in, making it an unlikely candidate for anoxia-mediated Ca^{2+} release. By similar reasoning, the Na^+-independent Ca^{2+} mechanism is hypothesized to exchange 2 H^+ for 1 Ca^{2+}, which is electroneutral and not influenced by changes in Ψ_m (Brand, 1985). This mechanism would require a reduction in $[H^+]_{matrix}$ to favour H^+ influx and Ca^{2+} efflux, but because mitochondrial H^+ extrusion *via* electron transport is halted during anoxia, the mechanism that would produce such a reduction is eliminated. It would therefore seem reasonable to investigate other potential Ca^{2+}-efflux pathways, the most curious one being the mitochondrial permeability transition pore (mPTP).

Often associated with mitochondrial damage and cell death, the most frequently investigated form of the mPTP is a mega-channel that forms a continuum between the inner and outer mitochondrial membranes in response to mitochondrial Ca^{2+} loading and allows passage of molecules of up to approximately 1.5 kDa (Haworth and Hunter, 1979). However, there also exists a low-conductance conformation of the mPTP that is permeable to small ions such as Ca^{2+} but impermeable to sucrose, making only molecules ~0.3 kDa or less able to cross the mitochondrial membranes (Hunter and Haworth, 1979b). This conformation is characterized by rapid and spontaneous fluctuations in Ψ_m, suggesting that the low-conductance conformation is used as an 'emergency mechanism' during oxidative stress and/or Ca^{2+} loading to release accumulated Ca^{2+} and to prevent prolonged mPTP opening and mitochondrial membrane rupture (Hüser and Blatter, 1999). This form of the mPTP has also been implicated in being involved in Ca^{2+} homeostasis during resting conditions, as myocyte mitochondria accumulate Ca^{2+} in the presence of the mPTP inhibitor cyclosporin A (CsA) (Altschuld et al., 1992). While Ca^{2+} loading appears to be the primary trigger of mPTP activation, its activity is also increased in the presence of reactive oxygen species, elevated phosphate, high pH and depolarized Ψ_m, while mPTP opening is antagonized by the presence of ATP/ADP, matrix Mg^{2+} and mitochondrial matrix pH <7.0 (Armstrong et al., 2003; Haworth and Hunter, 1979; Bernardi, 1992; Varanyuwatana and Halestrap, 2012). Because of the sensitivity of the mPTP to Ψ_m and the dependence of anoxia-mediated Ca^{2+} release on mK^+_{ATP} channels in turtle neurons, we hypothesized that the mitochondria rapidly release Ca^{2+} from the mitochondrial matrix following Ψ_m depolarization at the onset of anoxia through a low-conductance form of the mPTP and that this Ca^{2+} signal is used to attenuate NMDAR activity in the turtle cortex. Similar Ca^{2+} release mechanisms have been previously proposed (Hüser and Blatter, 1999), but this is the first study to investigate the mPTP as part of a neuroprotective mechanism that is responsible for NMDAR silencing. In this study, we report that NMDAR activity was reduced by Ca^{2+} release through the mPTP during anoxia, as Ca^{2+} release and NMDAR silencing during anoxia were abolished in a CsA-sensitive manner. This Ca^{2+} release mechanism was driven by depolarization of Ψ_m during anoxia, which occurred in response to opening of mK^+_{ATP} channels and was maintained at a new depolarized set-point by reverse activity of the F_1F_0-ATPase.

MATERIALS AND METHODS

Animal care and cortical slice preparation

This study was approved by the University of Toronto Animal Care Committee and conforms to the care and handling of animals as outlined in the Canadian Council on Animal Care's *Guide to the Care and Use of Experimental Animals*, Vol. 2. One hundred and nine adult turtles (*C. p. bellii*) with a mean (± s.d.) mass of 221±19 g were obtained from Niles Biological (Sacramento, CA, USA). Animals were housed in a large aquarium equipped with a flow-through freshwater system at 18°C, a non-aquatic basking platform and a heat lamp. Turtles were maintained on a 12 h:12 h light:dark photoperiod and were given access to food and water regularly.

Whole brains were rapidly excised from the cranium following decapitation. The entire dorsal cortex was dissected free and bathed in 3–5°C artificial turtle cerebrospinal fluid (aCSF) composed of (in mmol l^{-1}): 107 NaCl, 2.6 KCl, 1.2 $CaCl_2$, 1.0 $MgCl_2$, 2.0 NaH_2PO_4, 26.5 $NaHCO_3$, 10.0 glucose, 5.0 imidazole, pH 7.4; osmolarity 290–300 mOsM. Individual cortical sheets (2) were cut medially from the visual cortex of each cerebral hemisphere and subdivided into a total of six cortical sheets. One cortical sheet was used per experiment and a single neuron was recorded per sheet. Two cortical sheets were used per individual for any particular experiment, such that an N=10 consisted of five separate animals. Although not rigorously documented, tissue is routinely stored overnight in the refrigerator at 3–5°C. Responses to given treatments on the following day are not different than when tissue is tested on the same day as the dissection or when tissue was stored at room temperature (22°C) on the first day.

Whole-cell patch clamp recording protocol

Cortical sheets were placed on a coverslip in a perfusion chamber system (RC-26 open bath chamber with a P1 platform; Harvard Apparatus, Saint-Laurent, QC, Canada). The chamber was gravity perfused from a 1 litre glass bottle attached to an intravenous dripper that contained aCSF gassed with 95% O_2/5% CO_2 to achieve normoxic conditions. A second 1 litre glass bottle with an attached intravenous dripper contained aCSF gassed with 95% N_2/5% CO_2 to achieve anoxic perfusion. Anoxic aCSF tubing was double jacketed and the area between these jackets was gassed with 95% N_2/5% CO_2 to maintain anoxic conditions. A plastic cover with a hole for the electrode was placed over the saline bath and the space between the cover and the bath surface was gently gassed with 95% N_2/5% CO_2 during anoxic conditions. Experiments were conducted at room temperature (22°C).

Whole-cell recordings were performed using fire-polished 5–8 MΩ micropipettes produced from borosilicate glass capillary tubes and the P-97 micropipette puller model (Sutter Instruments, Novato, CA, USA). Pipette solution contained the following (in mmol l^{-1}): 8 NaCl, 0.003 $CaCl_2$, 10 Na-HEPES, 20 KCl, 110 potassium gluconate, 1 $MgCl_2$, 0.3 NaGTP and 2 NaATP (adjusted to pH 7.4 and osmolarity 290–300 mOsM). Cell-attached 1–20 GΩ seals were obtained using the blind-patch technique of Blanton et al. (Blanton et al., 1989). To break into the cell, the recording electrode potential was voltage-clamped to −80 mV and a sharp pulse of negative pressure was applied. Once the whole-cell configuration was established, cells were given at least 2 min to acclimate before series resistance was measured, which normally ranged from 20 to

100 MΩ. Patches were discarded if series resistance varied by >25% over the course of an experiment. Data were collected at 5–10 kHz using an Axopatch-1D amplifier, a CV-4 head stage and a Digidata 1200 interface (Molecular Devices, Sunnyvale, CA, USA) and then collected and stored on computer using Clampex 10 software (Molecular Devices). A fast-step perfusion system (VC-6 perfusion valve controller and SF-77B fast-step perfusion system; Harvard Apparatus) was used to deliver pharmacological agents to the tissue.

Neuronal cell identification

Neurons were identified as pyramidal or stellate based on the expressed electrophysiological properties, as outlined by Connors and Kriegstein (Connors and Kriegstein, 1986). Cells were current clamped and a current was injected for 450 ms to cause a 30 mV depolarizing change in membrane potential and action potential firing.

Whole-cell NMDAR current–voltage relationship

To assess the quality of the neuronal response to NMDA, a current–voltage relationship for NMDAR currents was obtained. After the patch has stabilized, the neuron was voltage-clamped to a holding potential of −80 mV and a 5-min perfusion of 1 μmol l^{-1} tetrodotoxin (TTX) (Cedarlane, Burlington, ON, Canada) was used to suppress action potentials. Cortical sheets were then perfused with 300 μmol l^{-1} NMDA until a current was elicited. The voltage of the patch-clamped neuron was then stepped from −100 to 40 mV in 10 mV increments. Typically, application of NMDA for 3–10 s was necessary to induce a response, which likely reflected the distance between the tip of the perfusion apparatus and the neuron. The same NMDA application time was then used for every subsequent recording performed on the same neuron within a single experiment.

Evoked NMDAR current recordings

Experiments were performed over 60 or 80 min periods, where NMDAR current recordings were made at t=0, 10, 40, 60 and 80 min and were performed as described above. Normoxic control NMDAR currents were recorded at t=0 min and at t=10 min. The initial recording at t=0 min was set to 100% and all subsequent recordings from that experiment were normalized to that control value, while the second control value at t=10 min was used for statistical analysis. Following the two control recordings, the tissue was perfused with anoxic aCSF or aCSF containing specific pharmacological compounds and evoked NMDAR currents were recorded after 30 and 50 min of treatment. Tissue was then re-perfused with control normoxic aCSF for 20 min and NMDAR currents were measured to demonstrate reversibility.

Fluorometric assessment of cytosolic Ca^{2+} changes

To assess cytosolic changes in [Ca^{2+}], cortical sheets were loaded with the Ca^{2+}-sensitive dye Oregon Green 488 BAPTA-1 AM (Life Technologies Inc., Burlington, ON, Canada). Two separate capped opaque vials contained 5 ml of aCSF and 5 μmol l^{-1} Oregon Green [from a 1 mmol l^{-1} Oregon Green stock solution in dimethyl sulfoxide (DMSO) and 20% pluronic acid] were prepared. Cortical sheets were loaded with Oregon Green for two consecutive 1 h incubations at 3–5°C in each separate vial, followed by a 20 min rinse in normal aCSF. Cortical sheets were incubated at 3–5°C to improve fluorescence intensity, as Oregon Green is rapidly extruded from cells *via* anion transport systems on the plasma membrane (Takahashi et al., 1999). Tissue that was incubated at room temperature exhibited a lower intensity than that incubated at 3–5°C (data not shown) but reacted to anoxia in the same manner. Following dye loading, slices were placed in a flow-through recording chamber equipped with the same perfusion system as the whole-cell patch clamp experiments. For experiments involving anoxia, a plastic cuff was placed around the objective and over the bath to provide constant N_2/CO_2 gas over the bath during anoxic exposure. For experiments assessing whether the origin of Ca^{2+} was intracellular or extracellular, aCSF containing 0 [Ca^{2+}] and 1 mmol l^{-1} ethylene glycol tetraacetic acid (EGTA) was used.

Oregon Green was excited at 488 nm using a DeltaRamX high-speed random access monochromator and an LPS-220B light source (Photon Technology International, London, ON, Canada) at a bandwidth of 4.5 nm using EastRatioPro software (Photon Technology International). Light passed through a shutter for 1 s prior to every recording. Fluorescence emission measurements were acquired at 10 s intervals using an Olympus BX51W1 microscope (Olympus Canada, Richmond Hill, ON, Canada) and Rolera-MGi Digital EMCCD camera (QImaging, Surrey, BC, Canada). Baseline fluorescence was first measured for ~10 min to achieve a stable baseline, followed by treatment exposure for periods of 10–30 min. Drugs were applied by bulk-perfusion as it was found that drug application using the fast-step perfusion system occasionally produced artificial increases in fluorescence intensity because the force of the flow of the incoming saline moved the tissue slightly and shifted the area of focus. Following each treatment, oxygenated control aCSF was perfused onto the tissue to allow fluorescence to return to baseline. Once each experiment was completed, aCSF flow was halted and tissues were incubated in 2 μmol ionomycin for 5 min, followed by introduction of 2 mmol l^{-1} $MnCl_2$, to quench the calcium fluorescence signal and obtain a value for background fluorescence. This value was subtracted from all recordings during analysis to isolate the fluorescence attributed to changes in [Ca^{2+}]. Changes in fluorescence were calculated as the difference between two parallel tangents obtained before and after treatment application and this value was divided by baseline fluorescence to obtain a percent change in calcium fluorescence. For each experimental recording, a minimum of 10 neurons were randomly chosen and the average change in Oregon Green fluorescence of these neurons was used as one N-value for statistical analysis. No observable changes in fluorescence occurred in response to anoxia in non-dye-loaded cells.

Fluorometric assessment of mitochondrial membrane potential

Cortical sheets were loaded with the mitochondrial trans-membrane-potential-sensitive dye rhodamine-123 (Invitrogen, Burlington, ON, Canada) in an opaque vial containing 5 ml aCSF and 50 μmol l^{-1} rhodamine-123 (from a 25 mmol l^{-1} rhodamine-123 stock solution in DMSO) for 50 min at 3–5°C, followed by a 20 min rinse in normal aCSF. Fluorescence measurements were conducted using the same equipment as the Oregon Green experiments. Rhodamine-123 was excited at 495 nm for 1 s prior to every recording, which was acquired at 5 s intervals.

Pharmacology

For electrophysiological measurements, 1 μmol l^{-1} TTX was delivered for 5 min prior to applying 300 μmol l^{-1} NMDA for 3–10 s and recording the evoked current. CNQX (6-cyano-7-nitroquinoxaline-2,3-dione; 25 μmol l^{-1}), gabazine (25 μmol l^{-1}) and CGP-55845 (5 μmol l^{-1}) were used to inhibit AMPARs, $GABA_A$ and $GABA_B$ receptors, respectively, to determine whether recorded NMDAR currents were purely due to NMDAR activation or also NMDAR-mediated activation of AMPARs or GABARs. Atractyloside (500 μmol l^{-1}), an mPTP opener, was applied for a

maximum of 20 min prior to recording, as application for longer periods induces irreversible apoptosis in rats (Isenberg and Klaunig, 2000). For experiments involving Ca^{2+} chelation, BAPTA (5 mmol l^{-1}) was included in the recording electrode solution. To inhibit mPTP opening activity, CsA (10 μmol l^{-1} from a stock dissolved in DMSO; LC Laboratories, Woburn, MA, USA), was diluted into turtle aCSF at volumes not exceeding 0.01% v/v and was bulk-perfused during all experiments. Prior to all experiments utilizing mPTP inhibition, tissue slices were incubated in aCSF containing 10 μmol l^{-1} CsA for a minimum of 30 min. The protonophore carbonyl cyanide-*p*-trifluoromethoxyphenylhydrazone (FCCP; 20 μmol l^{-1} from a stock solution dissolved in 95% ethanol) was applied to cause mitochondrial uncoupling and Ca^{2+} release. To test the effects of F_1F_0-ATPase inhibition, oligomycin was used (10 μmol l^{-1} from a stock dissolved in DMSO). mK^+_{ATP} channels were activated using the channel agonist diazoxide (100 μmol l^{-1} from a stock dissolved in DMSO) and blocked with the antagonist 5-HD (100 μmol l^{-1}). To test the effect of succinate dehydrogenase inhibition on rhodamine-123 fluorescence, malonate (5 mmol l^{-1}) was dissolved in turtle aCSF and bulk-perfused onto slices. Saline solutions containing drugs from DMSO-solubilized solutions were osmolarity-corrected to prevent hyper-osmotic conditions, as the addition of DMSO was found to increase osmolarity. All drugs, unless otherwise specified, were obtained from Sigma-Aldrich (Oakville, ON, Canada).

Statistical analysis

NMDAR whole-cell current data were analyzed following root arcsine transformation using a one-way repeated-measures ANOVA (Tukey test) to compare the means of normoxic controls and treatments within treatment groups. Oregon Green and rhodamine-123 fluorescence data were analyzed using a one-way ANOVA (Holm–Sidak method) following root arcsine transformation to compare the mean fluorescence between normoxic controls and treatments. Data *N*-values represent number of sheets/neurons analyzed per experimental data set.

RESULTS

NMDA receptor whole-cell current–voltage relationship

A current–voltage relationship for NMDARs in turtle pyramidal neurons was determined to confirm the receptor responded to NMDA in the characteristic N-shaped fashion, similar to its mammalian counterparts. Stepping the holding potential from −100 mV to +40 mV in the presence of 1 mmol l^{-1} Mg^{2+} yielded a reversal potential of approximately −6 mV and the voltage-dependent Mg^{2+} block of NMDARs was apparent at potentials of −40 mV or lower (Fig. 1). Mg^{2+} resides in the NMDAR pore at hyperpolarized potentials, thereby blocking conductance. This block is not present in the absence of extracellular Mg^{2+}, which results in a linear inward conductance at potentials more hyperpolarized than −40 mV (Shin and Buck, 2003).

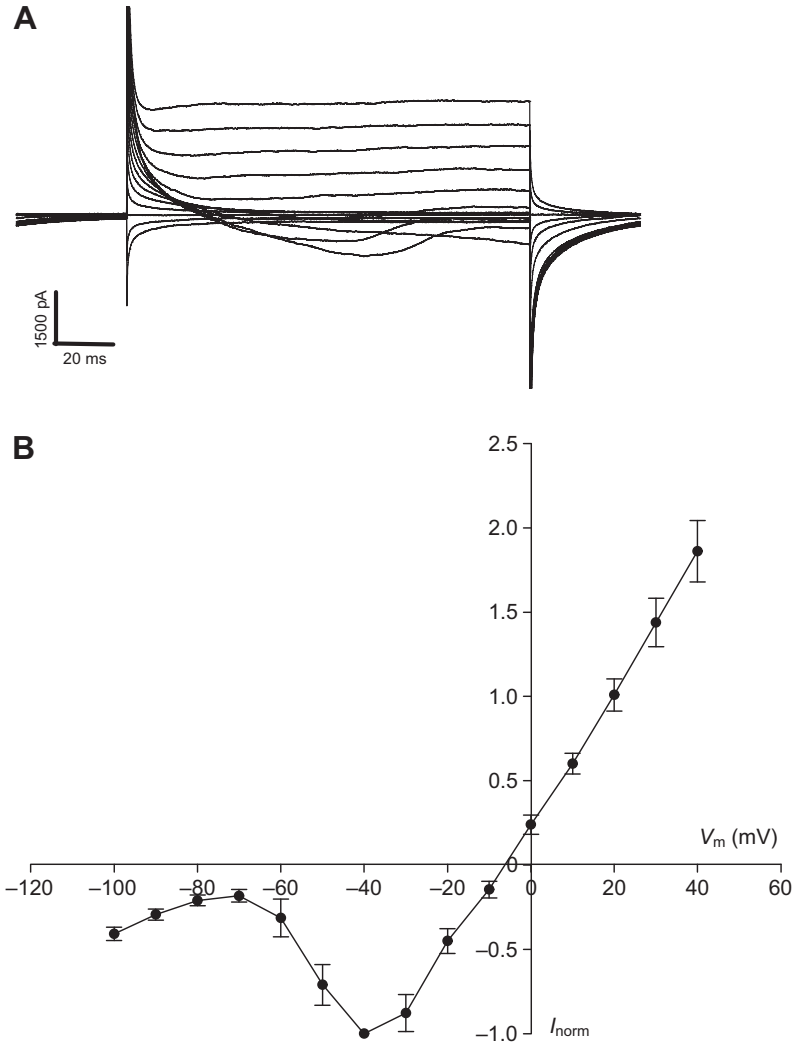

Fig. 1. Whole-cell NMDA receptor current–voltage relationship. (A) Sample trace of NMDAR currents from a neuron voltage-stepped from −100 to 40 mV. (B) NMDAR currents measured from −100 to 40 mV and normalized (I_{norm}) to current measured at −40 mV. Values were recorded in the presence of 1 mmol l^{-1} Mg^{2+} artificial cerebral spinal fluid and were not corrected for liquid-junction potential. V_m, membrane potential. Data are expressed as means ± s.e.m. (*N*=15).

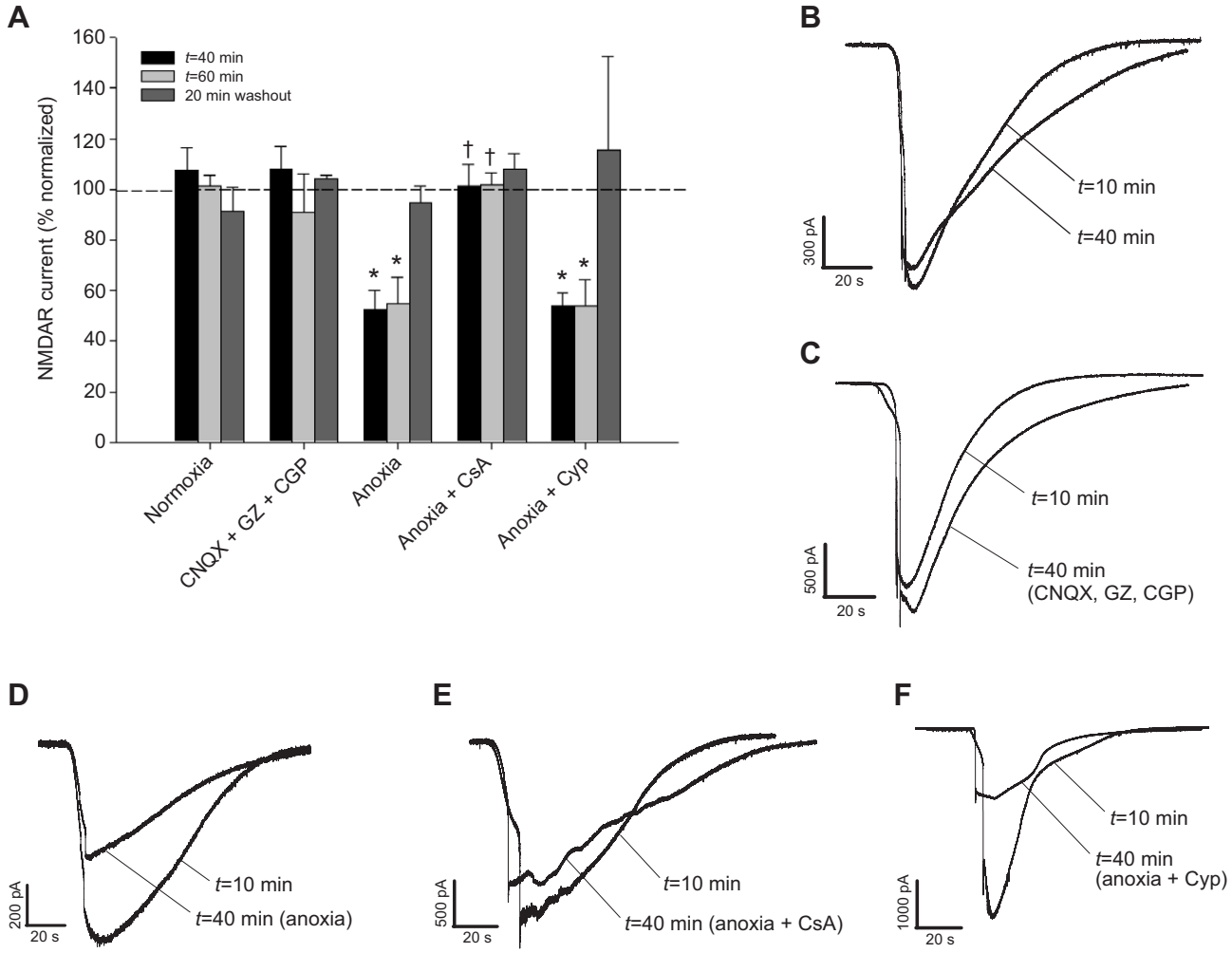

Fig. 2. NMDAR currents are reduced during anoxia and this reduction is blocked by inhibition of the mitochondrial permeability transition pore (mPTP) with cyclosporin A. (A) Percentage normalized NMDAR currents after 30 min (*t*=40 min, black bars) and 50 min (*t*=60 min, light grey bars) of treatment, followed by 20 min of washout (dark grey bars). The dashed line represents normoxic controls taken at *t*=10 min (*N*=47). Symbols indicate data significantly different from normoxic controls taken at *t*=10 min (*) and anoxic controls taken at corresponding time points (†) (*P*<0.05). Data are expressed as means ± s.e.m. (B–F) Paired sample NMDAR currents at *t*=10 min (control) and following 30 min of anoxic or pharmacological treatment exposure (*t*=40 min). CNQX, 6-cyano-7-nitroquinoxaline-2,3-dione; GZ, gabazine; CGP, CGP-55845; CsA, cyclosporin A; Cyp, cypermethrin.

mPTP activation reduces NMDAR activity during normoxia and inhibition blocks NMDAR silencing during anoxia

Normoxic NMDAR currents were stable and did not change significantly over the 80 min experimental period [107.02±7.47% (*N*=10) at *t*=40 min, 105.53±5.36% (*N*=8) at *t*=60 min, and 95.41±5.63% (*N*=5) at *t*=80 min; Fig. 2A,B]. Typical NMDAR current responses varied from ~1.0 to 2.0 nA in amplitude. To confirm that AMPA and GABA receptors did not contribute to the NMDA-evoked currents in the presence of TTX, AMPA receptors were antagonized using CNQX, and $GABA_A$ and $GABA_B$ receptors were antagonized using gabazine and CGP-55845, respectively. AMPAR/GABAR inhibition did not significantly alter NMDA-evoked currents after 30 min (108.13±8.81%, *N*=6) or 50 min (90.84±15.32%, *N*=3; Fig. 2A,C), suggesting that the measured currents are specifically due to NMDAR activation. Following the onset of anoxia, NMDAR currents decreased to 52.58±7.37% (*N*=9, *P*<0.05) and 55.00±10.11% (*N*=5, *P*<0.05) of normoxic control values at *t*=40 and 60 min, respectively, and was fully reversible to normoxic levels after 20 min of re-oxygenation (94.52±6.83%, *N*=4; Fig. 2A,D). This agrees with previous studies investigating anoxia-mediated NMDAR channel arrest (Shin and Buck, 2003; Pamenter et al., 2008b). Anoxic conditions in the recording chamber after 30 min of anoxic saline perfusion were confirmed using an oxygen electrode (data not shown).

To determine whether the mPTP is a necessary component of the channel arrest mechanism, 10 μmol l^{-1} CsA was used to inhibit mPTP opening during anoxic conditions. Inclusion of CsA in the bulk perfusate completely abolished the anoxia-mediated reduction in NMDAR currents after 30 and 50 min of anoxia (101.60±8.28%, *N*=10 and 101.70±5.00%, *N*=9, respectively; Fig. 2A,E). No change in NMDAR currents was observed following re-oxygenation (107.80±6.46%, *N*=8). An inherent quality of CsA is that it is non-specific and inhibits calcineurin, a protein phosphatase (Liu et al., 1991). To prove that the reduction in NMDAR currents is not due to this pharmacological side effect, 500 nmol l^{-1} cypermethrin was used to inhibit calcineurin during anoxic conditions. Inhibition of calcineurin did not affect the reduction in NMDAR currents after 30 or 50 min

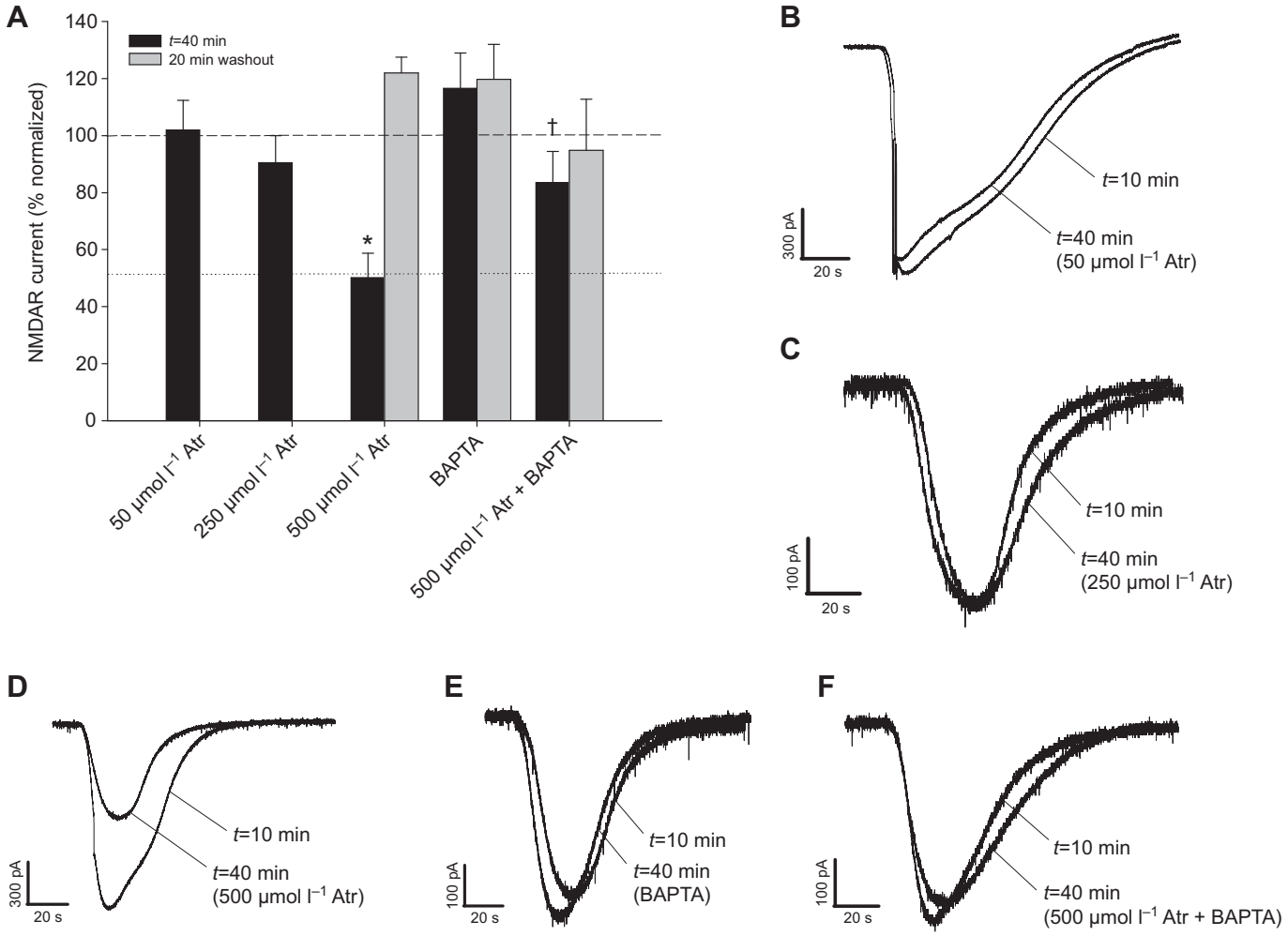

Fig. 3. Activation of the mitochondrial permeability transition pore with atractyloside reduces NMDAR currents in a Ca^{2+}-dependent manner. (A) Percentage normalized NMDAR currents after 30 min (*t*=40 min, black bars) followed by 20 min of washout (grey bars). The dashed line represents normoxic controls taken at *t*=10 min (*N*=47) and the dotted line represents anoxic controls taken at *t*=40 min (*N*=9). Symbols indicate data significantly different from normoxic controls taken at *t*=10 min (*) and drug treatment controls taken at *t*=40 min (†) ($P<0.05$). Data are expressed as means ± s.e.m. (B–F) Paired sample NMDAR currents at *t*=10 min (control) and following 30 min of treatment exposure (*t*=40 min). Atr, atractyloside; BAPTA, 1,2-bis(o-aminophenoxy)ethane-*N*,*N*,*N*′,*N*′-tetraacetic acid.

of anoxia (53.94±5.09%, *N*=6 and 54.10±10.06, *N*=4, respectively; Fig. 2A,F), and this effect is also reversible following re-oxygenation (115.6±37.01%, *N*=3), suggesting that the abolishment of anoxia-mediated NMDAR current reduction using CsA is a result of mPTP inhibition.

To investigate whether activation of the mPTP during normoxia could reduce NMDAR activity as a result of Ca^{2+} release, an appropriate concentration of atractyloside for mPTP activation was first determined. Concentrations of atractyloside vary across studies, ranging from 10 to 100 µmol l^{-1} in isolated mitochondria to 200 µmol l^{-1} to 2 mmol l^{-1} in whole tissue slices (Asimakis and Sordahl, 1977; Obatomi et al., 1998). During normoxia, opening of the mPTP with 50 or 250 µmol l^{-1} atractyloside had no effect on NMDAR currents (93.30±7.53%, *N*=5 and 100.66±11.35%, *N*=4, respectively; Fig. 3A–C) but decreased to 50.11±8.68% of normoxic control values (*N*=6, $P<0.05$) after application of 500 µmol l^{-1} atractyloside (Fig. 3A,D). This effect was reversed following 20 min of drug washout with aCSF (121.96±5.63%, *N*=6) at *t*=60 (Fig. 3A). To confirm that the atractyloside-mediated NMDAR silencing effect was a result of mitochondrial Ca^{2+} release and not due to Ca^{2+}-independent pharmacological modulation of NMDARs, 5 mmol l^{-1} BAPTA was included in the pipette solution. Inclusion of BAPTA alone did not have an effect on NMDAR receptor currents during normoxia at *t*=40 min (116.55±12.51%, *N*=6) or at *t*=60 min (119.73±12.24%, *N*=6; Fig. 3A,E), but it abolished the atractyloside-mediated reduction in NMDAR currents during normoxia at *t*=40 min (83.51±10.99%, *N*=5, $P<0.05$; Fig. 3A,F). Washout of atractyloside when BAPTA was included in the pipette solution at *t*=60 min (94.91±17.89%, *N*=3) did not differ from experiments without BAPTA (Fig. 3A,F), suggesting that the atractyloside-mediated reduction in NMDAR currents is a Ca^{2+}-dependent phenomenon.

mPTP activation increases $[Ca^{2+}]_c$ during normoxia and mPTP inhibition attenuates the anoxia-mediated rise in $[Ca^{2+}]_c$

To examine the role of mPTP opening on mitochondrial calcium release, we used the calcium-sensitive dye Oregon Green to study relative changes in $[Ca^{2+}]_c$ during anoxia and pharmacological manipulation of the mPTP. Under normoxic conditions, Oregon Green fluorescence did not significantly change with respect to

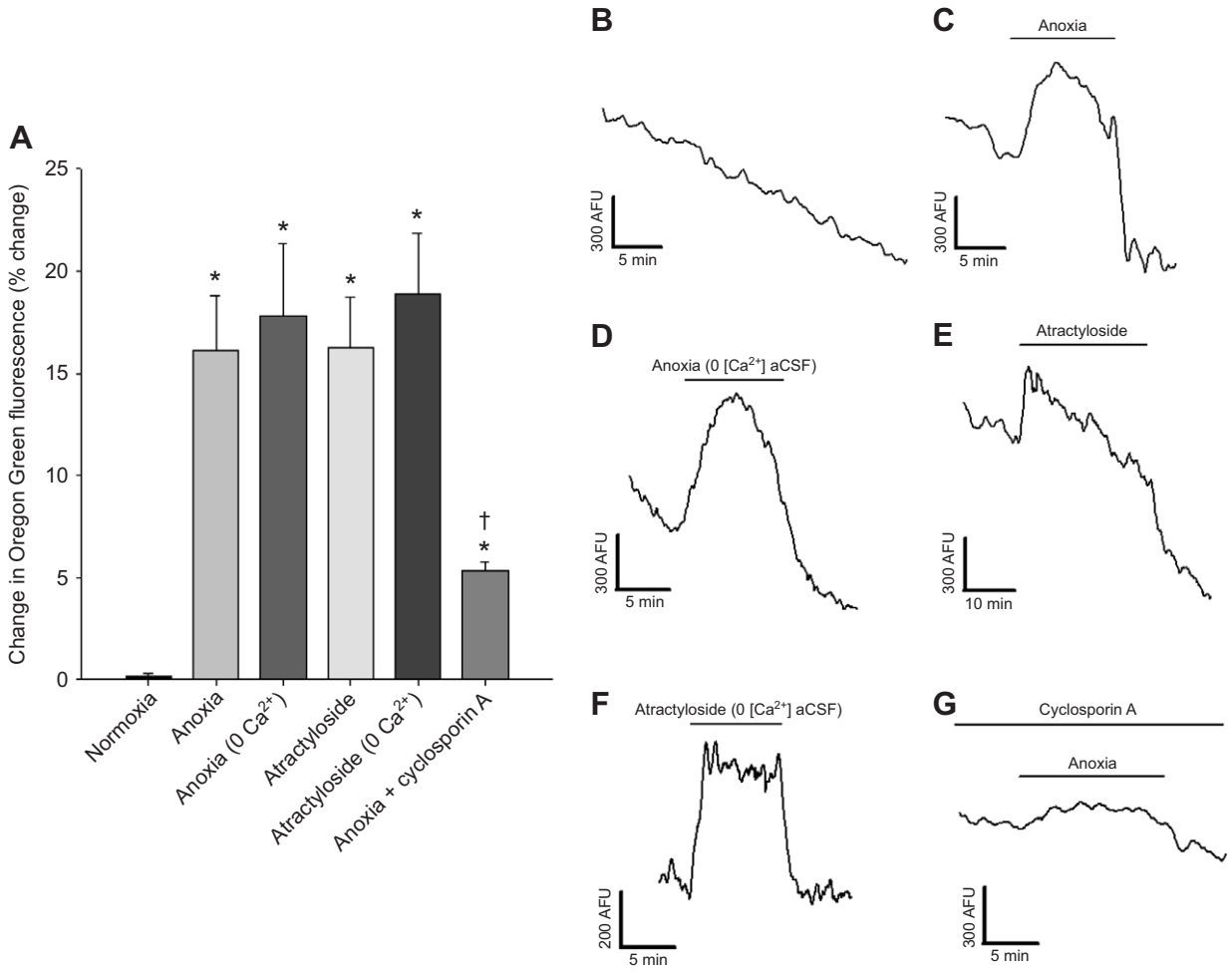

Fig. 4. Oregon Green [Ca^{2+}] fluorescence increases in response to anoxia and mPTP activation. (A) Percentage normalized changes in Oregon Green fluorescence post treatment. Symbols indicate values different from normoxic controls (*) or anoxic controls (†) (P<0.05). All data are expressed as means ± s.e.m. (B–G) Sample data traces of Oregon Green fluorescence from single-neuron regions of interest, treated as indicated. Traces were smoothed using EasyRatioPro software to eliminate noise-related artifacts. AFU, arbitrary fluorescence unit; aCSF, artificial cerebral spinal fluid.

its baseline (0.19±0.10% increase from baseline, N=9; Fig. 4A,B) and decreased at a steady rate because of photo-bleaching and/or dye exocytosis. Following the onset of anoxia, Oregon Green fluorescence increased by 16.13±2.67% (N=8, P<0.05; Fig. 4A,C). This increase in Ca^{2+}-induced fluorescence was still observed in the absence of extracellular Ca^{2+} (17.79±3.52%, N=4, P<0.05; Fig. 4A,D), which, in accordance with previous observations (Pamenter et al., 2008b), demonstrates that the increased [Ca^{2+}] during anoxia is caused by release from an intracellular source. To investigate whether this increase in Ca^{2+} is due to release through the mPTP, opening of the mPTP was stimulated with atractyloside during normoxic conditions. These conditions also produced an increase in Ca^{2+} levels (16.25±2.25%, N=7, P<0.05; Fig. 4A,E), and this increase of Ca^{2+} fluorescence following atractyloside application was still observed in the absence of extracellular Ca^{2+} (18.85±3.03%, N=7, P<0.05; Fig. 4A,F). Inclusion of the mPTP blocker CsA in the bulk perfusate during anoxic conditions attenuated Oregon Green fluorescence to a 5.33±0.40% increase from baseline, and this was significantly different from both anoxic and normoxic control values (N=8, P<0.05; Fig. 4A,G). Application of DMSO vehicle alone during anoxia (11.76±0.44%, N=4) did not significantly affect Ca^{2+} fluorescence from the anoxic level. These data suggest that mPTP opening is involved in the anoxia-mediated calcium release mechanism that is required for NMDAR downregulation.

Mitochondrial membrane potential is depolarized following anoxia or pharmacological activation of the mPTP

To examine whether Ψ_m is maintained or depolarized during anoxia and pharmacological manipulation of the mPTP, we utilized the Ψ_m-sensitive dye rhodamine-123. Under normoxic conditions, rhodamine-123 fluorescence did not significantly change with respect to its baseline (0.39±0.12%, N=7; Fig. 5A,B) and decreased at a steady rate because of photobleaching and/or dye exocytosis. In response to anoxic conditions, fluorescence increased by 6.56±0.97% (N=9, P<0.05; Fig. 5A,C), suggesting a depolarization of Ψ_m. To investigate whether opening the mPTP during normoxia influences Ψ_m in a manner similar to anoxia, 500 μmol l^{-1} atractyloside was used. Atractyloside application resulted in a significant fluorescence increase compared with normoxic controls (6.36±0.95%, N=6, P<0.05; Fig. 5A,E). Inclusion of the mPTP inhibitor CsA in the bulk perfusate attenuated the anoxia-mediated increase in fluorescence to 3.53±0.53% of baseline values, and these were significantly different from normoxic controls but not anoxic

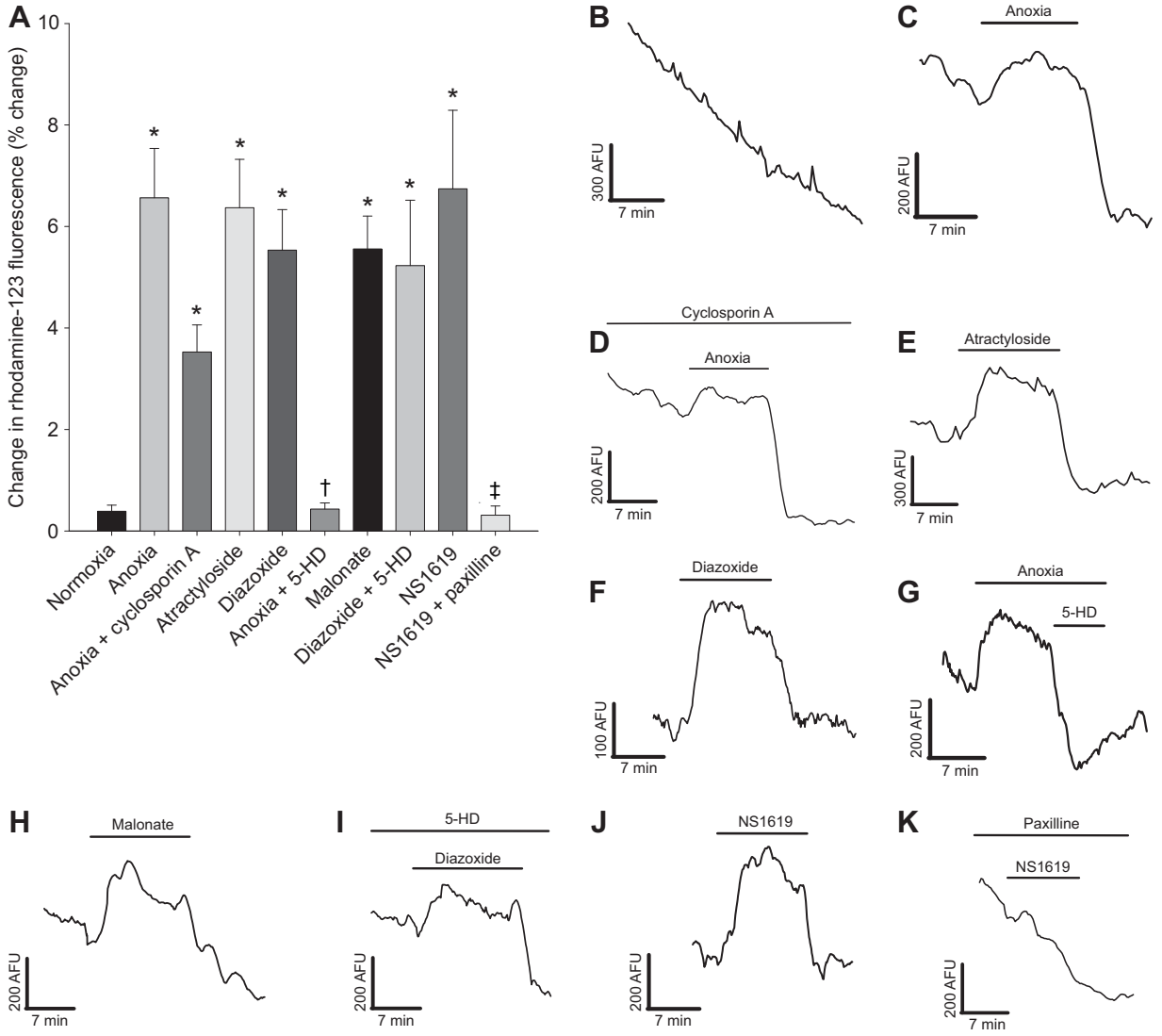

Fig. 5. Rhodamine-123 Ψ_m fluorescence increases in response to anoxia and is dependent on mK^+_{ATP} channel activation, but not mPTP activity. (A) Percentage normalized changes in rhodamine-123 fluorescence post treatment. Symbols indicate values different from normoxic controls (*), anoxic controls (†) or NS1619 controls (‡) (P<0.05). All data are expressed as means ± s.e.m. (B–K) Sample data traces of rhodamine-123 fluorescence from single-neuron regions of interest, treated as indicated. Traces were smoothed using EasyRatioPro software to eliminate noise-related artifacts. AFU, arbitrary fluorescence unit; 5-HD, 5-hydroxydecanoic acid.

values (N=6, P<0.05; Fig. 5A,D), suggesting that Ψ_m depolarization occurs upstream of mPTP opening.

Uncoupling the mitochondria with a proton ionophore following anoxia results in additional calcium release and collapse of Ψ_m

It is of interest to understand how an anoxia-tolerant organism releases mitochondrial calcium stores without undergoing irreversible mitochondrial damage. In response to ischemia, mammalian cardiac tissue experiences infarct damage in response to lowered oxygen levels, mitochondrial depolarization/swelling and release of apoptotic factors *via* high-conductance mitochondrial permeability (Halestrap et al., 2004). We therefore hypothesized that turtle neurons experience a regulated depolarization of Ψ_m, resulting in mild mitochondrial depolarization/uncoupling and calcium release driven down its electrochemical gradient. To test this hypothesis, Oregon Green dye-loaded turtle neurons were exposed to anoxic conditions and allowed to recover before exposure to the proton ionophore FCCP. Application of FCCP resulted in a 70.21±13.52% (N=5, P<0.05; Fig. 6A,B) increase in Ca^{2+} fluorescence, which is approximately fourfold greater than Ca^{2+} fluorescence caused by anoxic conditions (16.12±2.66%, N=8). Similarly, FCCP caused a 62.96±12.00% increase in rhodamine-123 fluorescence (P<0.05; Fig. 7A,B), which is approximately ninefold greater than the anoxia-mediated increase in rhodamine fluorescence (6.56±0.97%, N=9). These and the Ca^{2+} fluorescence data together suggest that mitochondrial membrane potential is carefully regulated at a depolarized state under anoxic conditions.

Mildly depolarized state of anoxic mitochondria is maintained *via* opening of mK^+_{ATP} channels and reversal of the F_1F_0-ATPase

To confirm that mK^+_{ATP} channel opening is responsible for the anoxia-mediated release of Ca^{2+} by matrix depolarization, we studied the effects of mK^+_{ATP} channel modulators on Ψ_m. Activation

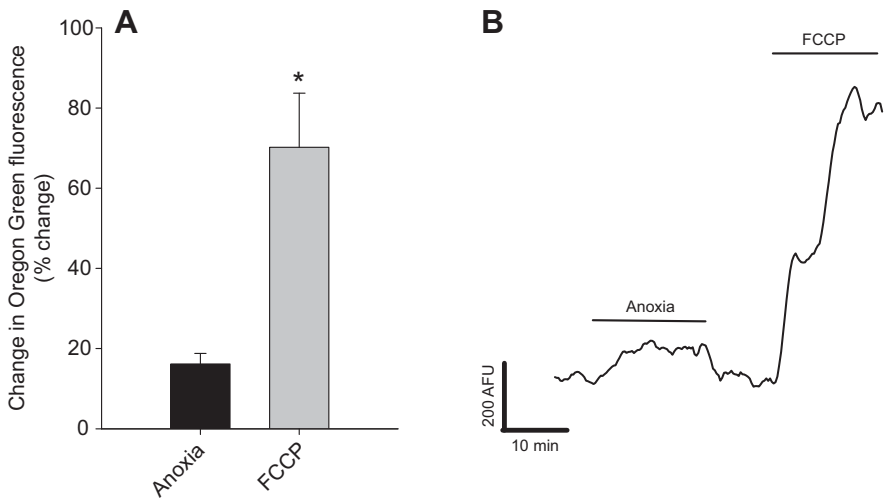

Fig. 6. Additional mitochondrial calcium is released following anoxia in response to mitochondrial uncoupling. (A) Normalized proportional changes in Oregon Green calcium fluorescence following treatment exposure (N=5, P<0.05). Each value was allowed to recover from anoxia to baseline before FCCP application. Symbols indicate significant changes from anoxic controls (*P<0.05). (B) Sample data trace of Oregon Green fluorescence from a single-neuron region of interest, treated as indicated. Traces were smoothed using EasyRatioPro software to eliminate noise-related artifacts.

of these channels with 100 µmol l^{-1} diazoxide during normoxia resulted in a 5.53±0.79% (N=7, P<0.05; Fig. 5A,F) increase in rhodamine-123 fluorescence, while mK^+_{ATP} channel blockade with 100 µmol l^{-1} 5-HD abolished the anoxia-mediated rise in rhodamine-123 fluorescence (0.43±0.12%, N=5, P<0.05; Fig. 5A,G). The effects of diazoxide cannot be considered to be purely due to mK^+_{ATP} channel activation, however, as it could not be blocked by 100 µmol l^{-1} 5-HD (7.92±2.85%, N=4, P<0.05, Fig. 5A,I). This effect could possibly be due to inhibition of succinate dehydrogenase (SDH), as SDH inhibition with 5 mmol l^{-1} malonate produced a 5.56±0.64% increase in rhodamine-123 fluorescence (N=6, P<0.05; Fig. 5A,H). To provide evidence that the increase in rhodamine-123 fluorescence is due to an inward mitochondrial K^+ current, we utilized the calcium-activated mitochondrial potassium (mK^+_{Ca}) channel activator NS1619. Application of NS1619 during normoxic conditions produced a 6.74±1.54% (N=4, P<0.05; Fig. 5A,J) increase in rhodamine-123 fluorescence, which was blocked in the presence of the mK^+_{Ca} inhibitor paxilline (0.31±0.18%, N=4, P<0.05; Fig. 5A,K).

The anoxia-tolerant frog *Rana temporaria* is able to maintain the mitochondrial proton gradient during anoxia by hydrolyzing ATP *via* the F_1F_0-ATPase (St-Pierre et al., 2000). We were therefore interested in testing whether the turtle utilizes a similar mechanism to maintain Ψ_m during anoxic periods. We found that exposing anoxic turtle neurons to the F_1F_0-ATPase-inhibitor oligomycin (20 µmol l^{-1}) resulted in a 33.69±6.81% (N=8, P<0.05; Fig. 7A,C) increase in rhodamine-123 fluorescence. At elevated concentrations, oligomycin is also a potent inhibitor of the plasmalemmal Na^+/K^+-ATPase (Homareda et al., 2000). To show that the oligomycin-mediated rise in rhodamine-123 fluorescence is not an artifactual side effect of destabilizing Na^+ and K^+ gradients, we applied 1 mmol l^{-1} ouabain following the anoxia-mediated rise in rhodamine-123 fluorescence. No significant deviations from the anoxia-mediated rise in rhodamine-123 fluorescence were observed in the presence of ouabain (8.67±1.05%, N=5; Fig. 7A) or a DMSO vehicle (7.70±2.30%, N=3; Fig. 7A). Taken together, these data suggest that reversal of the F_1F_0-ATPase counteracts the inward K^+ current through mK^+_{ATP} channels and maintains Ψ_m at a new depolarized set-point.

DISCUSSION

In this investigation, we demonstrated that the rise in $[Ca^{2+}]_i$ in turtle neurons during anoxia is in part due to Ca^{2+} release from the mitochondria through the mPTP. This conclusion was reached based on the inhibition of mPTP opening using CsA, which blocked both the mitochondrial release of Ca^{2+} and the reduction in NMDAR currents during anoxia. Conversely, stimulation of mPTP opening using atractyloside during normoxic conditions resulted in a rise in $[Ca^{2+}]_i$ and reduction of NMDAR currents. We concluded that mPTP opening occurs in response to Ψ_m depolarization at the onset of anoxia, as the anoxia-mediated depolarization of Ψ_m can be blocked with the mK^+_{ATP} channel blocker 5-HD or simulated with diazoxide during normoxic conditions. Because application of the protonophore FCCP depolarized Ψ_m beyond the anoxic baseline, we concluded that Ψ_m is being maintained at a mildly depolarized set-point by some unknown mechanism. The F_1F_0-ATPase inhibitor oligomycin produced an effect similar to that of FCCP, which led us to the conclusion that the newly set Ψ_m during anoxia was maintained by H^+ efflux *via* the F_1F_0-ATPase (Fig. 8).

Mitochondrial calcium release and subsequent NMDAR current reduction occurs in response to, but is not specific to, Ψ_m depolarization *via* mK^+_{ATP} channel activation

While the mechanism proposed in this study centres around mPTP activation by conductance through mK^+_{ATP} channels, activation of the mK^+_{ATP} channel is not a necessary attribute for mitochondrial Ca^{2+} release. Downregulation of NMDAR conductance in turtle neurons also occurs following treatment of NS1619 and can be blocked in the presence of paxilline (Pamenter et al., 2008b). Further evidence that supports this observation was shown in this study, where NS1619 produced a depolarization of Ψ_m that could be blocked by paxilline. Taking this evidence into consideration, it suggests that Ca^{2+} release from the mitochondria is not specific to which channel is actually being activated but rather by the depolarizing effect that is elicited. This is in agreement with the hypothesis that mPTP activation occurs following Ψ_m depolarization but independently of matrix Ca^{2+} load (Bernardi, 1992).

In spite of this, however, the mK^+_{ATP} channel remains the most likely candidate for this mechanism because of its sensitivity to [ATP]. Its connection to Ca^{2+} release during energy crisis has also been observed in isolated rat cardiac mitochondria, as diazoxide reduced the driving force for Ca^{2+} uptake through the Ca^{2+} uniporter yet also resulted in reduced accumulation of Ca^{2+} through an undetermined efflux mechanism (Holmuhamedov et al., 1999). This Ca^{2+} efflux mechanism was found to be CsA sensitive, which corroborates our hypothesis of coupling mK^+_{ATP} channel activation to mPTP-mediated Ca^{2+} release.

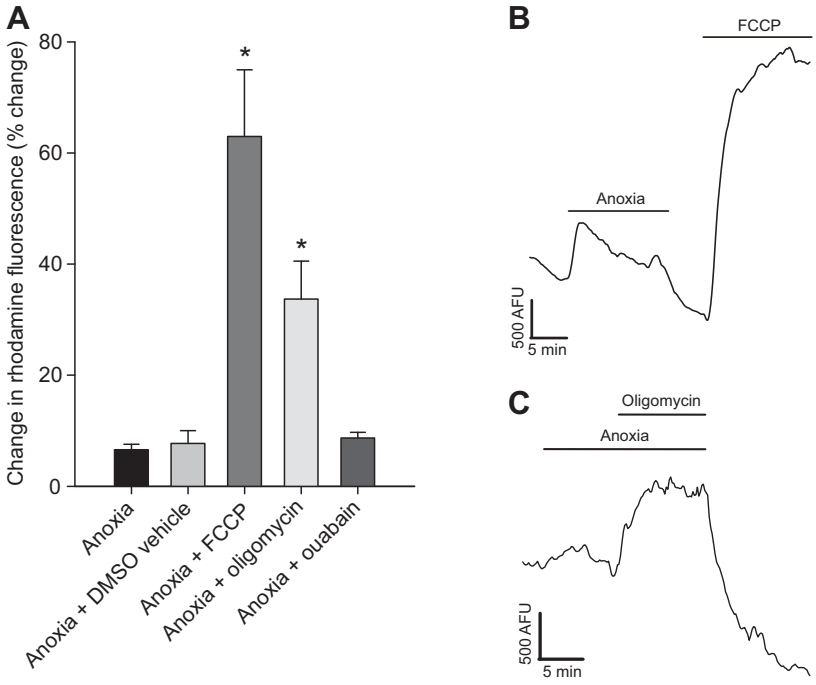

Fig. 7. Mitochondrial membrane potential (Ψ_m) is depolarized further than the anoxic level following mitochondrial uncoupling or F_1F_0-ATPase inhibition during anoxia. (A) Changes in rhodamine-123 fluorescence following treatment exposure, relative to the anoxic fluorescence level. Each value was allowed to recover from anoxia to baseline before pharmacological applications. Symbols indicate significant changes from anoxic controls (*P<0.05). (B,C) Sample data traces of rhodamine-123 fluorescence from single-neuron regions of interest, treated as indicated. Traces were smoothed using EasyRatioPro software to eliminate noise-related artifacts.

Alternative mechanisms to the mPTP for calcium release from the mitochondria

It is possible that the turtle brain has alternative measures of anoxic Ca^{2+} efflux from the mitochondria, as CsA did not completely block Ca^{2+} release: Pamenter et al. (Pamenter et al., 2008b) hypothesized that during anoxia, mK^+_{ATP} channel activation depolarizes the mitochondrial membrane potential and reduces the driving force for Ca^{2+} influx through the Ca^{2+} uniporter, resulting in an accumulation of $[Ca^{2+}]_c$. The uncertainty surrounding this hypothesis stems from the uniporter as a Ca^{2+} efflux avenue. Although current through this channel is driven by Ψ_m and can be directed extra-mitochondrially following Ψ_m depolarization, activation requires elevated extra-mitochondrial $[Ca^{2+}]_c$ and Ca^{2+} binding to an activator site, a condition only possible through cell stimulation (Montero et al., 2001). The study presented here, and that performed by Pamenter et al. (Pamenter et al., 2008b), found a rise in $[Ca^{2+}]_c$ in response to anoxia in the absence of extracellular Ca^{2+}. Furthermore, inhibition of Ca^{2+} efflux from the endoplasmic reticulum does not attenuate NMDAR currents (Pamenter et al., 2008b), suggesting that Ca^{2+}-induced Ca^{2+} release from the mitochondria in response to endoplasmic reticulum stimulation is not a likely possibility. In spite of eliminating all extra-mitochondrial Ca^{2+} sources, mitochondrial Ca^{2+} release still occurs. Because Ca^{2+} binding to a site on the uniporter is necessary for channel conductance, it therefore seems unlikely that Ca^{2+} efflux occurs through the uniporter in response to anoxia. However, the slow rise in Ca^{2+} fluorescence in the presence of CsA illustrated in Fig. 4G suggests that Ca^{2+} efflux may be occurring through an inwardly rectifying channel, a property that the uniporter possesses (Kirichok et al., 2004). In addition, Ca^{2+} efflux through Na^+-dependent/-independent exchangers is unlikely

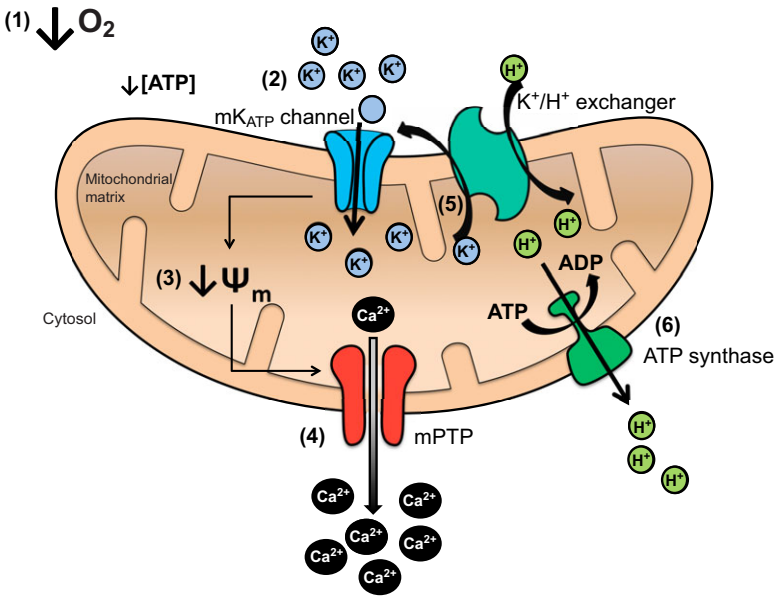

Fig. 8. Simplified schematic illustrating how lowered oxygen tension results in mitochondrial calcium release. The absence of cellular O_2 leads to a halt in ATP production *via* oxidative phosphorylation (1). This results in a reduction in local [ATP] at the mitochondrial membrane, which stimulates mK^+_{ATP} channel opening and increases K^+ conductance into the mitochondrial matrix (2). This consequentially depolarizes Ψ_m (3), which triggers transient opening of the mPTP and Ca^{2+} release (4). While mK^+_{ATP} channels remain constitutively open, $[K^+]_{mitochondrial}$ is balanced by K^+/H^+ exchange (5). The imbalance in $[H^+]$ is itself maintained by reversal of the F_1F_0-ATPase (ATP synthase) (6), which prevents collapse of the proton gradient while maintaining Ψ_m at a newly depolarized set point. Reintroduction of O_2 would halt this pathway by oxidatively producing ATP, resulting in mK^+_{ATP} channel closure, reestablishment of Ψ_m and closure of the mPTP.

because its driving force is believed to be dependent on increases in matrix Na^+, H^+ or Ψ_m hyperpolarization (Gunter et al., 2000), conditions that are unlikely to occur during anoxia. Taking this evidence into consideration, the most reasonable mechanism for mitochondrial Ca^{2+} release occurs in response to either regulated mitochondrial permeability or a currently unknown mechanism.

Conditions supporting low-conductance mPTP opening in the anoxic turtle brain

A major controller of mitochondrial pore formation is intracellular/matrix pH, as isolated mitochondria exposed to solutions of pH 6.0 exhibit less than 10% of CsA-inhibited mitochondrial permeability of those exposed to pH 7.4 (Halestrap, 1991). While lowered pH is typically associated with hypoxic/anoxic conditions, the turtle's extraordinary buffering capacity allows it to maintain extracellular pH above 7.0 for at least 3 weeks of anoxia at 3°C (Ultsch and Jackson, 1982). Such alkaline conditions would favour mPTP formation if they are also produced intracellularly and would serve to reduce NMDAR currents during short-term anoxia. Following a 3 week span, NMDAR regulation shifts from one of post-translational modification to one of subunit expression as NR1 abundance is reduced to 40% of normoxic levels (Bickler et al., 2000). Another strong regulator of the mPTP is adenylate phosphate concentrations, as removal of ADP from cellular media induces mitochondrial permeability (Hunter and Haworth, 1979a). Unlike mammalian models, the turtle brain maintains cellular [ATP] after 1 h of anoxia before experiencing a modest decrease in cellular [ATP] to ~70% of control values after 2 h of anoxia (Buck et al., 1998). During this time, micro-domains of the cell may be prone to changes in [ATP] at sites with high ATPase density. We propose that such local fluctuations of [ATP] at the mitochondrial membrane during oxygen deprivation could activate mK^+_{ATP} channels, but global maintenance of [ATP] remains high enough to prevent high-conductance mitochondrial permeability.

Pharmacological modulation of the mPTP using commercially available agents

To date, the structure of the mPTP remains unclear. A number of theories have been proposed: one suggests a protein complex composed of the mitochondrial proteins including the adenine nucleotide translocase (ANT), voltage-dependent anion channel (VDAC) and cyclophilin-D (Cyp-D), although this is problematic as mitochondrial permeability occurs in ANT-knockout or $VDAC1^{-/-}$ mitochondria from mice (Javadov et al., 2009; Kokoszka et al., 2004; Krauskopf et al., 2006). Others have suggested that the mitochondrial phosphate carrier or ATP synthase form protein complexes that produce mitochondrial permeation (Varanyuwatana and Halestrap, 2012; Giorgio et al., 2013). Regardless of which of these theories proves correct, there are a number of pharmacological agents that have been found to regulate mitochondrial permeability. Atractyloside functions as an inhibitor of the ANT by locking it into a permeability-favouring conformation that halts ATP/ADP transport. For this reason, it is typically used in cellular toxicity assays or as an uncoupling agent, and few electrophysiological studies have been performed in its presence. It was therefore necessary to exclude the possibility of direct modulation of NMDARs by atractyloside. This was achieved by including BAPTA in the patch pipette to chelate Ca^{2+} released in response to atractyloside application to reverse the calcium-dependent attenuation of NMDAR currents. Reversal of the atractyloside-mediated reduction in NMDAR currents in the presence of BAPTA tells us that (1) the atractyloside-mediated reduction in NMDAR currents was calcium-mediated and (2) atractyloside did not reduce NMDAR currents by directly modulating NMDARs or by activating calcium-independent second messenger pathways that would modulate NMDARs. Furthermore, it illustrates that a rise in $[Ca^{2+}]_i$ is sufficient to reduce NMDAR currents in the absence of oxygen stress.

CsA functions by competitively binding to Cyp-D, a peptidyl prolyl isomerase (PPIase) localized to the mitochondrial matrix. Binding occurs at its isomerase active site, thereby eliminating its activity (Walsh et al., 1992). This is unfortunately not a ubiquitous pathway, as inhibition of mPTP activation using CsA is ineffective in some organisms, such as yeast (Jung et al., 1997) and *Drosophila* (von Stockum et al., 2011). In the present study, incubation of neurons in 10 μmol l^{-1} CsA attenuated Ca^{2+} release and blocked the anoxia-mediated reduction in NMDAR currents, suggesting that activation of the mPTP by Cyp-D plays a role in anoxia-mediated Ca^{2+} release. It is possible that its failure to completely block Ca^{2+} release from turtle mitochondria is due to a lack of drug specificity to the mPTP complex, but there is no evidence to bolster this point. Nevertheless, while we showed that CsA attenuated Ca^{2+} release and 5-HD also blocks Ca^{2+} release (Pamenter et al., 2008b), the inability of CsA to completely block Ψ_m depolarization while 5-HD did suggests that depolarization occurs prior to mPTP opening *via* mK^+_{ATP} channel activation.

A central concern in any study utilizing CsA is its non-specific binding characteristics. CsA unselectively binds to cellular cyclophilins, a family of proteins exhibiting PPIase activity. The most abundant member of this family is the cytosolic protein cyclophilin A, which, when bound to CsA, produces a complex that inhibits the calcium-/calmodulin-dependent phosphatase 2B, also known as calcineurin (Walsh et al., 1992). Inhibition of calcineurin produces immunosuppressive effects by impeding the conversion of T cells from a quiescent to an activated state and blocking transcriptional activation of genes responsible for the inflammatory response (Walsh et al., 1992). While the immunosuppressive effects of CsA are unlikely to be an issue in this particular study, calcineurin inactivation may play a more important role. Calcineurin desensitizes the NMDAR response by modulating the NR2A subunit at the intracellular C terminus through de-phosphorylation of serine and tyrosine residues (Krupp et al., 2002). This could potentially destabilize the interaction between the NMDAR and the actin cytoskeleton, resulting in a reduction in NMDAR activity, as actin depolymerisation induces NMDAR rundown (Rosenmund and Westbrook, 1993). Because of its role in NMDAR regulation, the effect of calcineurin in anoxic turtle neurons has been previously investigated: calcineurin inhibition using cypermethrin did not prevent anoxia from suppressing NMDAR activity after 2 h in turtle neurons (Bickler et al., 2000). However, in a separate study, cypermethrin application eliminated anoxia-mediated silencing of NMDAR activity after 20 min, but not 40 min, of anoxia (Shin et al., 2005). In the present study, it was found that cypermethrin did not prevent NMDAR silencing after 30 or 50 min of anoxia and therefore cannot be considered a side effect of CsA application.

A role for ATP synthase in the anoxic brain

An interesting recent development indicates that the molecular identity of the mPTP could be a dimerized complex of mitochondrial ATP synthase, as it is capable of producing currents of a mitochondrial mega-channel that can be inhibited by ADP but not by CsA (Giorgio et al., 2013). The importance of the ATP synthase during oxygen stress may not only be as a component of the mPTP but also to prevent collapse of Ψ_m, as illustrated in this study. Here,

it was found that inhibition of the ATP synthase with oligomycin resulted in a collapse of Ψ_m in a manner similar to that of the protonophore FCCP. This finding is not exclusive to the turtle, as ATP consumption by the ATP synthase comprises ~9% of ATP utilized during anoxia in frog skeletal muscle, despite a reduction in enzymatic activity (St-Pierre et al., 2000). Using changes of pH in mitochondrial suspensions as a measure of F_1F_0-ATPase activity, St-Pierre et al. (St-Pierre et al., 2000) concluded that ATPase activity is reduced during anoxic conditions, leading to reduced Ψ_m from lowered proton efflux and a consequent decrease in driving force for proton leak. Thus, a reduction in proton leakage reduces the need to consume ATP to re-establish proton gradients. The reverse activity of the ATP synthase in both turtles and frogs suggests that this pathway could be ubiquitous across anoxia-tolerant species and may be central to the mitochondrial mechanisms of anoxia tolerance.

Concluding remarks

In conclusion, our study illustrates that the mitochondria play an integral part in the turtle's ability to withstand oxygen deprivation through NMDAR current silencing by releasing Ca^{2+} through a CsA-sensitive mPTP. While the most commonly cited function of the mPTP is apoptotic induction, this is the first study to demonstrate indirectly that Ca^{2+} release through the mPTP regulates NMDAR activity in a neuroprotective fashion. By further investigating this Ca^{2+}-release pathway, it may be possible to develop an understanding about what separates low- and high-conductance mitochondrial permeability mechanisms and how this pathway can be exploited for controlling neuronal excitability without compromising mitochondrial function.

LIST OF ABBREVIATIONS

5-HD	5-hydroxydecanoic acid
aCSF	artificial cerebral spinal fluid
AFU	arbitrary fluorescence unit
AMPA	2-amino-3-(3-hydroxy-5-methyl-isoxazol-4-yl)propanoic acid
ANT	adenine nucleotide translocase
Atr	atractyloside
BAPTA	1,2-bis(o-aminophenoxy)ethane-*N*,*N*,*N*',*N*'-tetraacetic acid
CGP	CGP-55845
CNQX	6-cyano-7-nitroquinoxaline-2,3-dione
CsA	cyclosporin A
Cyp	cypermethrin
Cyp-D	cyclophilin D
DMSO	dimethyl sulfoxide
EGTA	ethylene glycol tetraacetic acid
FCCP	carbonyl cyanide-*p*-trifluoromethoxyphenylhydrazone
GZ	gabazine
mK^+_{ATP}	mitochondrial ATP-sensitive potassium
mK^+_{Ca}	calcium-activated mitochondrial potassium
mPTP	mitochondrial permeability transition pore
NMDA	*N*-methyl-D-aspartate
NMDAR	NMDA receptor
PPIase	peptidyl prolyl isomerase
SDH	succinate dehydrogenase
TTX	tetrodotoxin
VDAC	voltage-dependent anion channel
Ψ_m	mitochondrial membrane potential

ACKNOWLEDGEMENTS

The authors would like to thank to Professors Michael Salter and Melanie Woodin for insightful critique of acquired data during the early stages of this study.

AUTHOR CONTRIBUTIONS

L.T.B. contributed to the conception and design of the experiments performed in this study, provided all equipment and materials required to perform the study, and assisted in interpreting data and revising the article. P.J.H. contributed to the conception and design of the experiments performed in this study, the execution and interpretation of all findings presented in this article, and drafting and revising the article.

COMPETING INTERESTS

No competing interests declared.

FUNDING

This study was funded by the Natural Sciences and Engineering Research Council [NSERC Discovery Grant] to L.T.B. and an Ontario Graduate Scholarship [QEII] to P.J.H.

REFERENCES

Altschuld, R. A., Hohl, C. M., Castillo, L. C., Garleb, A. A., Starling, R. C. and Brierley, G. P. (1992). Cyclosporin inhibits mitochondrial calcium efflux in isolated adult rat ventricular cardiomyocytes. *Am. J. Physiol.* **262**, H1699-H1704.

Armstrong, J. S., Whiteman, M., Rose, P. and Jones, D. P. (2003). The coenzyme Q_{10} analog decylubiquinone inhibits the redox-activated mitochondrial permeability transition – role of mitochondrial respiratory complex III. *J. Biol. Chem.* **278**, 49079-49084.

Asimakis, G. K. and Sordahl, L. A. (1977). Effects of atractyloside and palmitoyl coenzyme A on calcium transport in cardiac mitochondria. *Arch. Biochem. Biophys.* **179**, 200-210.

Baysal, K., Jung, D. W., Gunter, K. K., Gunter, T. E. and Brierley, G. P. (1994). Na^+-dependent Ca^{2+} efflux mechanism of heart mitochondria is not a passive $Ca^{2+}/2Na^+$ exchanger. *Am. J. Physiol.* **266**, C800-C808.

Bernardi, P. (1992). Modulation of the mitochondrial cyclosporin A-sensitive permeability transition pore by the proton electrochemical gradient. Evidence that the pore can be opened by membrane depolarization. *J. Biol. Chem.* **267**, 8834-8839.

Bickler, P. E., Donohoe, P. H. and Buck, L. T. (2000). Hypoxia-induced silencing of NMDA receptors in turtle neurons. *J. Neurosci.* **20**, 3522-3528.

Blanton, M. G., Lo Turco, J. J. and Kriegstein, A. R. (1989). Whole cell recording from neurons in slices of reptilian and mammalian cerebral cortex. *J. Neurosci. Methods* **30**, 203-210.

Brand, M. D. (1985). Electroneutral efflux of Ca^{2+} from liver mitochondria. *Biochem. J.* **225**, 413-419.

Buck, L. T. and Bickler, P. E. (1995). Role of adenosine in NMDA receptor modulation in the cerebral cortex of an anoxia-tolerant turtle (*Chrysemys picta belli*). *J. Exp. Biol.* **198**, 1621-1628.

Buck, L. T. and Bickler, P. E. (1998). Adenosine and anoxia reduce *N*-methyl-D-aspartate receptor open probability in turtle cerebrocortex. *J. Exp. Biol.* **201**, 289-297.

Buck, L. T. and Hochachka, P. W. (1993). Anoxic suppression of Na^+-K^+-ATPase and constant membrane potential in hepatocytes: support for channel arrest. *Am. J. Physiol.* **265**, R1020-R1025.

Buck, L. T., Espanol, M., Litt, L. and Bickler, P. (1998). Reversible decreases in ATP and PCr concentrations in anoxic turtle brain. *Comp. Biochem. Physiol.* **120A**, 633-639.

Choi, D. W. (1992). Excitotoxic cell death. *J. Neurobiol.* **23**, 1261-1276.

Connors, B. W. and Kriegstein, A. R. (1986). Cellular physiology of the turtle visual cortex: distinctive properties of pyramidal and stellate neurons. *J. Neurosci.* **6**, 164-177.

Giorgio, V., von Stockum, S., Antoniel, M., Fabbro, A., Fogolari, F., Forte, M., Glick, G. D., Petronilli, V., Zoratti, M., Szabó, I. et al. (2013). Dimers of mitochondrial ATP synthase form the permeability transition pore. *Proc. Natl. Acad. Sci. USA* **110**, 5887-5892.

Gunter, T. E., Buntinas, L., Sparagna, G., Eliseev, R. A. and Gunter, K. K. (2000). Mitochondrial calcium transport: mechanisms and functions. *Cell Calcium* **28**, 285-296.

Halestrap, A. P. (1991). Calcium-dependent opening of a non-specific pore in the mitochondrial inner membrane is inhibited at pH values below 7. Implications for the protective effect of low pH against chemical and hypoxic cell damage. *Biochem. J.* **278**, 715-719.

Halestrap, A. P., Clarke, S. J. and Javadov, S. A. (2004). Mitochondrial permeability transition pore opening during myocardial reperfusion – a target for cardioprotection. *Cardiovasc. Res.* **61**, 372-385.

Haworth, R. A. and Hunter, D. R. (1979). The Ca^{2+}-induced membrane transition in mitochondria. II. Nature of the Ca^{2+} trigger site. *Arch. Biochem. Biophys.* **195**, 460-467.

Hochachka, P. W. (1986). Defense strategies against hypoxia and hypothermia. *Science* **231**, 234-241.

Holmuhamedov, E. L., Wang, L. and Terzic, A. (1999). ATP-sensitive K^+ channel openers prevent Ca^{2+} overload in rat cardiac mitochondria. *J. Physiol.* **519**, 347-360.

Homareda, H., Ishii, T. and Takeyasu, K. (2000). Binding domain of oligomycin on Na^+,K^+-ATPase. *Eur. J. Pharmacol.* **400**, 177-183.

Hunter, D. R. and Haworth, R. A. (1979a). The Ca^{2+}-induced membrane transition in mitochondria. I. The protective mechanisms. *Arch. Biochem. Biophys.* **195**, 453-459.

Hunter, D. R. and Haworth, R. A. (1979b). The Ca^{2+}-induced membrane transition in mitochondria. III. Transitional Ca^{2+} release. *Arch. Biochem. Biophys.* **195**, 468-477.

Hüser, J. and Blatter, L. A. (1999). Fluctuations in mitochondrial membrane potential caused by repetitive gating of the permeability transition pore. *Biochem. J.* **343**, 311-317.

Isenberg, J. S. and Klaunig, J. E. (2000). Role of the mitochondrial membrane permeability transition (MPT) in rotenone-induced apoptosis in liver cells. *Toxicol. Sci.* **53**, 340-351.

Javadov, S., Karmazyn, M. and Escobales, N. (2009). Mitochondrial permeability transition pore opening as a promising therapeutic target in cardiac diseases. *J. Pharmacol. Exp. Ther.* **330**, 670-678.
Jung, D. W., Bradshaw, P. C. and Pfeiffer, D. R. (1997). Properties of a cyclosporin-insensitive permeability transition pore in yeast mitochondria. *J. Biol. Chem.* **272**, 21104-21112.
Kirichok, Y., Krapivinsky, G. and Clapham D. E. (2004). The mitochondrial calcium uniporter is a highly selective ion channel. *Nature* **427**, 360-364.
Kokoszka, J. E., Waymire, K. G., Levy, S. E., Sligh, J. E., Cai, J., Jones, D. P., MacGregor, G. R. and Wallace, D. C. (2004). The ADP/ATP translocator is not essential for the mitochondrial permeability transition pore. *Nature* **427**, 461-465.
Krauskopf, A., Eriksson, O., Craigen, W. J., Forte, M. A. and Bernardi, P. (2006). Properties of the permeability transition in VDAC1$^{-/-}$ mitochondria. *Biochim. Biophys. Acta* **1757**, 590-595.
Krupp, J. J., Vissel, B., Thomas, C. G., Heinemann, S. F. and Westbrook, G. L. (2002). Calcineurin acts via the C-terminus of NR2A to modulate desensitization of NMDA receptors. *Neuropharmacology* **42**, 593-602.
Liu, J., Farmer, J. D., Jr, Lane, W. S., Friedman, J., Weissman, I. and Schreiber, S. L. (1991). Calcineurin is a common target of cyclophilin-cyclosporin A and FKBP-FK506 complexes. *Cell* **66**, 807-815.
Montero, M., Alonso, M. T., Albillos, A., García-Sancho, J. and Alvarez, J. (2001). Mitochondrial Ca^{2+}-induced Ca^{2+} release mediated by the Ca^{2+} uniporter. *Mol. Biol. Cell* **12**, 63-71.
Nicholls, D. G. and Budd, S. L. (2000). Mitochondria and neuronal survival. *Physiol. Rev.* **80**, 315-360.
Obatomi, D. K., Thanh, N. T. K., Brant, S. and Bach, P. H. (1998). The toxic mechanism and metabolic effects of atractyloside in precision-cut pig kidney and liver slices. *Arch. Toxicol.* **72**, 524-530.
Pamenter, M. E., Shin, D. S. and Buck, L. T. (2008a). AMPA receptors undergo channel arrest in the anoxic turtle cortex. *Am. J. Physiol.* **294**, R606-R613.
Pamenter, M. E., Shin, D. S., Cooray, M. and Buck, L. T. (2008b). Mitochondrial ATP-sensitive K^+ channels regulate NMDAR activity in the cortex of the anoxic western painted turtle. *J. Physiol.* **586**, 1043-1058.
Pek-Scott, M. and Lutz, P. L. (1998). ATP-sensitive K^+ channel activation provides transient protection to the anoxic turtle brain. *Am. J. Physiol.* **275**, R2023-R2027.
Pérez-Pinzón, M. A., Rosenthal, M., Sick, T. J., Lutz, P. L., Pablo, J. and Mash, D. (1992). Downregulation of sodium channels during anoxia: a putative survival strategy of turtle brain. *Am. J. Physiol.* **262**, R712-R715.
Rodgers-Garlick, C. I., Hogg, D. W. and Buck, L. T. (2013). Oxygen-sensitive reduction in Ca^{2+}-activated K^+ channel open probability in turtle cerebrocortex. *Neuroscience* **237**, 243-254.
Rosenmund, C. and Westbrook, G. L. (1993). Calcium-induced actin depolymerization reduces NMDA channel activity. *Neuron* **10**, 805-814.
Shin, D. S. and Buck, L. T. (2003). Effect of anoxia and pharmacological anoxia on whole-cell NMDA receptor currents in cortical neurons from the western painted turtle. *Physiol. Biochem. Zool.* **76**, 41-51.
Shin, D. S.-H., Wilkie, M. P., Pamenter, M. E. and Buck, L. T. (2005). Calcium and protein phosphatase 1/2A attenuate N-methyl-D-aspartate receptor activity in the anoxic turtle cortex. *Comp. Biochem. Physiol.,* **142**, 50-57.
St-Pierre, J., Brand, M. D. and Boutilier, R. G. (2000). Mitochondria as ATP consumers: cellular treason in anoxia. *Proc. Nat. Acad. Sci.* **97**, 8670-8674.
Takahashi, A., Camacho, P., Lechleiter, J. D. and Herman, B. (1999). Measurement of intracellular calcium. *Physiol. Rev.* **79**, 1089-1125.
Thompson, J. W., Prentice, H. M. and Lutz, P. L. (2007). Regulation of extracellular glutamate levels in the long-term anoxic turtle striatum: coordinated activity of glutamate transporters, adenosine, K (ATP) (+) channels and GABA. *J. Biomed. Sci.* **14**, 809-817.
Ultsch, G. R. and Jackson, D. C. (1982). Long-term submergence at 3°C of the turtle, *Chrysemya picta bellii*, in normoxic and severely hypoxic water: I. Survival, gas exchange and acid-base status. *J. Exp. Biol.* **96**, 11-28.
Varanyuwatana, P. and Halestrap, A. P. (2012). The roles of phosphate and the phosphate carrier in the mitochondrial permeability transition pore. *Mitochondrion* **12**, 120-125.
von Stockum, S., Basso, E., Petronilli, V., Sabatelli, P., Forte, M. A. and Bernardi, P. (2011). Properties of Ca^{2+} transport in mitochondria of *Drosophila melanogaster*. *J. Biol. Chem.* **286**, 41163-41170.
Walsh, C. T., Zydowsky, L. D. and McKeon, F. D. (1992). Cyclosporin A, the cyclophilin class of peptidylprolyl isomerases, and blockade of T cell signal transduction. *J. Biol. Chem.* **267**, 13115-13118.